

Accepted Manuscript

Studies on N-picolinoyl-N'-benzothioylhydrazide and its Zn(II) complex: Synthesis, structure, antibacterial activity, thermal analysis and DFT calculation

S.K. Kushawaha, R.K. Dani, M.K. Bharty, U.K. Chaudhari, V.K. Sharma, R.N. Kharwar, N.K. Singh

PII: S0022-2860(14)00077-5

DOI: <http://dx.doi.org/10.1016/j.molstruc.2014.01.043>

Reference: MOLSTR 20320

To appear in: *Journal of Molecular Structure*

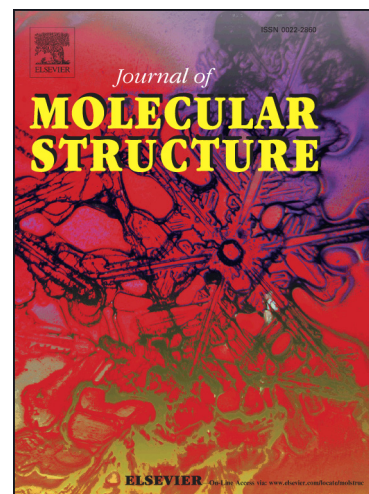
Received Date: 16 November 2013

Revised Date: 15 January 2014

Accepted Date: 15 January 2014

Please cite this article as: S.K. Kushawaha, R.K. Dani, M.K. Bharty, U.K. Chaudhari, V.K. Sharma, R.N. Kharwar, N.K. Singh, Studies on N-picolinoyl-N'-benzothioylhydrazide and its Zn(II) complex: Synthesis, structure, antibacterial activity, thermal analysis and DFT calculation, *Journal of Molecular Structure* (2014), doi: <http://dx.doi.org/10.1016/j.molstruc.2014.01.043>

This is a PDF file of an unedited manuscript that has been accepted for publication. As a service to our customers we are providing this early version of the manuscript. The manuscript will undergo copyediting, typesetting, and review of the resulting proof before it is published in its final form. Please note that during the production process errors may be discovered which could affect the content, and all legal disclaimers that apply to the journal pertain.



**Studies on N-picolinoyl-N'-benzothioylhydrazide and its Zn(II) complex:
Synthesis, structure, antibacterial activity, thermal analysis and DFT
calculation**

S.K. Kushawaha^a, R.K. Dani^a, M.K. Bharty^{a*}, U.K. Chaudhari^a, V.K. Sharma^b, R.N. Kharwar^b, N.K. Singh^{a*}

^aDepartment of Chemistry, ^bDepartment of Botany, Faculty of Science, Banaras Hindu University, Varanasi-221005, India

Abstract

A new Zn(II) complex [Zn(pbth)₂] (where Hpbth = N-picolinoyl-N'-benzothioylhydrazide) has been synthesized and characterized by elemental analyses, IR, UV-Visible and single crystal X-ray data. The distorted octahedral complex [Zn(pbth)₂] crystallizes in monoclinic system with space group C 2/c and is stabilized by various types of inter and intramolecular extended hydrogen bonding providing supramolecular framework. The optimized molecular geometry of N-picolinoyl-N'-benzothioylhydrazide (Hpbth) and the zinc complex in the ground state have been calculated by using the DFT method using B3LYP functional with 6-311 G(d,p){C,H,N,O,S}/Lanl2DZ basis set. The results of the optimized molecular geometry are presented and compared with the experimental X-ray diffraction data. In addition, quantum chemical calculations of Hpbth and the complex, molecular electrostatic potential (MEP), contour map and frontier molecular orbital analysis were performed. The solid state electrical conductivity and thermal behavior (TGA) of the complex were investigated. The bioefficacy of the complex has been examined against the growth of bacteria *in vitro* to evaluate their anti-microbial potential.

Keywords: NNS donor ligand, Zn(II) complex, Supramolecular architecture, Bactericidal property, DFT calculation.

*Corresponding author. Tel.: +91 542 6702447, E-mail: mkbharty@bhu.ac.in (M.K. Bharty), singhnk_bhu@yahoo.com (N.K. Singh)

1. Introduction

N'-Thioaroyl derivatives of acyl hydrazine are the next higher homolog of potential biologically important compounds after semicarbazides and thiosemicarbazides which is due to their flexibility in assuming different conformations [1-3]. They display beneficial biological activities, such as antitumor, antibacterial, antiviral and antimalarial activities [4-7]. The biological activities of these compounds are considered to be due to the presence of HNCS moiety and their ability to form chelates with metal ions. Biological activities of metal complexes generally differ from those of either ligands or the metal ions and the changes in biological activities are reported for several transition metal complexes [8, 9]. Furthermore, the above type of ligands can coordinate either in the neutral or in the anionic form because of the possibility of tautomerism which makes their study extremely interesting [10]. Due to the presence of potential donor sites, N'-aroyl derivatives of thiocarbohydrazides are interesting ligands and generate mononuclear, dinuclear and even tetranuclear complexes which provide a new dimension to supramolecular chemistry [11, 12]. Investigations into the structural stability of these compounds using both experimental techniques and theoretical methods have been of interest for many years. In view of this, we have synthesized and characterized the Zn(II) complex of a new NNS tridentate ligand N-picolinoylN'-benzothioylhydrazide. DFT calculation, thermal behavior, electrical conductivity has been studied. The antimicrobial properties of the ligand and the Zn(II) complex have also been examined against the growth of several bacterial pathogens.

2. Experimental

2.1. Chemicals and starting materials

Commercial reagents were used without further purification. Picolinic acid hydrazide (Sigma Aldrich), $\text{Zn}(\text{OAc})_2 \cdot 2\text{H}_2\text{O}$ (BDH Chemicals) were used as received. Carboxymethyl dithiobenzoate was prepared by the reported method [13]. All the synthetic manipulations were carried out in open atmosphere and at room temperature. The solvents were distilled before use following the standard procedure.

2.2. Physical measurements

Carbon, hydrogen, nitrogen and sulphur contents were estimated on a CHN Model CE-440 Analyzer and on an Elementar Vario EL III Carlo Erba 1108. IR spectra were recorded in the $4000\text{--}400\text{ cm}^{-1}$ region as KBr pellets on a Varian Excalibur 3100 FT-IR spectrophotometer. ^1H and ^{13}C NMR spectra were recorded in $\text{DMSO-}d_6$ on a JEOL AL300 FT-NMR spectrometer using TMS as internal reference. Electrical conductance of pressed pellets was measured by a conventional two-probe method in the 312-443 K range with contacts made on the pellet surfaces by means of silver paint. A Keithley 236 SMU was used to measure the sample resistance. Thermogravimetric analysis of the complex was done using a Perkin Elmer-STA 6000 thermal analyser in a nitrogen atmosphere at a heating rate of $15\text{ }^\circ\text{C min}^{-1}$.

2.3 Antibacterial tests

Five human bacterial pathogens *Salmonella typhi* (MTCC 3216), *Shigella flexneri* (ATCC 12022), *Staphylococcus aureus* (ATCC 25323), *Aeromonas hydrophila* (ATCC 7966) and *Enterococcus faecalis* were used to test the antibacterial activity of the ligand, $\text{Zn}(\text{OAc})_2 \cdot 2\text{H}_2\text{O}$ and the zinc complex. The antibacterial assay was done according to the reported method [14]

with some slight modifications [15]. The test compounds were dissolved in DMSO to a final concentration of 5 mg/ml. Sterilized Whatman no. 1 filter paper discs (5 mm) were impregnated with different volume (1, 2, 4, 6, 8 and 10 μ L) of compounds to get a final concentration of 5, 10, 20, 30, 40 and 50 μ g per disc. Sterilized paper disc loaded with the 10 μ L of DMSO was taken as a control. The bacterial test pathogens were spread on fresh Mueller Hinton Agar (MHA) plates with the help of cotton swabs to form an even lawn of the test bacteria. The filter paper disc impregnated with the test compound were placed on the surface of the MHA plates seeded with test bacteria and the plates were incubated in a B. O. D. incubator (Caltan-152, Narang Scientific Works, New Delhi, India) for 24 h at 37 ± 2 °C. The inhibition zones around each disc were measured after 24 h of incubation. Commercial antibacterial drugs streptomycin sulphate and neomycin sulphate (Himedia) were used in same concentration of 5-50 μ g/disc to compare effectiveness of the test compounds.

2.4. Synthesis

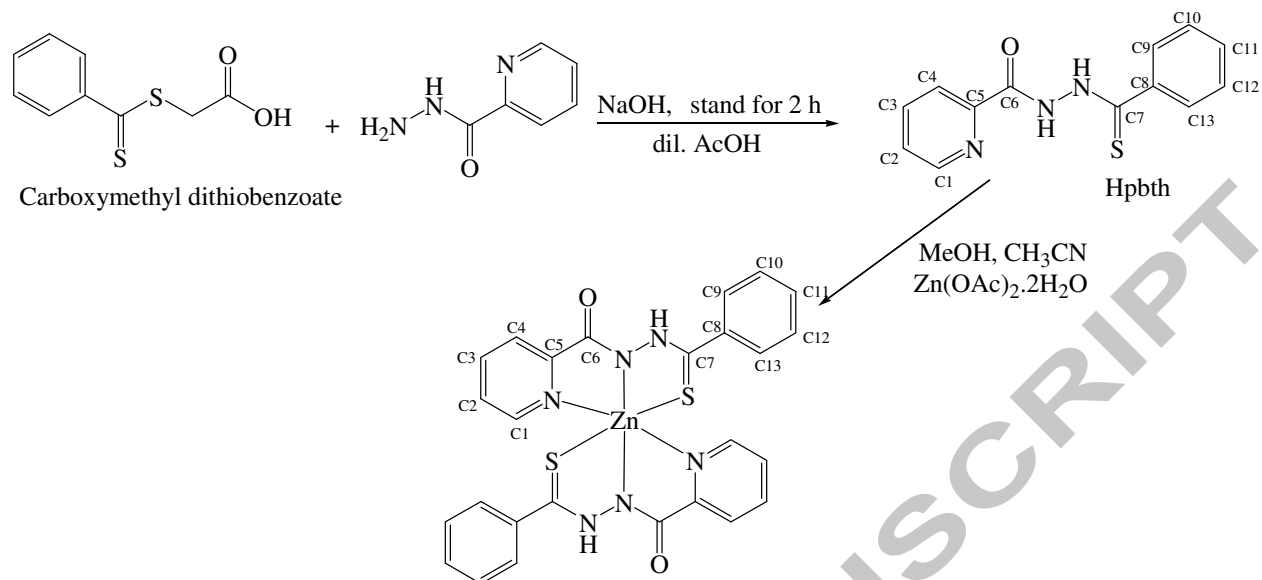
2.4.1. Synthesis of *N*-picolinoyl-*N'*-benzothioylhydrazide (*Hpbth*)

N-picolinoyl-*N'*-benzothioylhydrazide (*Hpbth*) was prepared by adding a methanol solution of carboxymethyl dithiobenzoate (2.12 g, 10 mmol) dropwise to 1N NaOH solution of picolinic acid hydrazide (1.37 g, 10 mmol). The reaction mixture was stirred continuously for 1 h and acidified with dil. acetic acid. The precipitate obtained was filtered off, washed with water, dried under reduced pressure and recrystallized from a mixture of MeOH-CHCl₃ (50:50 v/v) [16]. Yield: 75 %; m.p. 184 °C. Found: C, 60.73; H, 4.31; N, 16.30; S, 12.47 %. Calc. for C₁₃H₁₁N₃SO (257.31): C, 60.70; H, 4.28; N, 16.33; S, 12.44 %. IR (cm⁻¹, KBr): ν (N-H) 3236; ν (C=O) 1661; ν (N-N) 1075; ν (C=S) 921. ¹H NMR (DMSO-*d*₆; δ ppm): 10.63, 10.05 (s, 2H, NH), 8.68 (C1H), 7.90 (C2H), 7.92 (C3H), 8.044 (C4H), 7.65 (C9H), 7.36 (C10H), 7.34 (C11H),

7.22 (C12H), 7.50 (C13H), ^{13}C NMR (DMSO- d_6 ; δ ppm): 190.71 (C=S), 163.07 (C=O), 147.53 (C1), 131.17 (C2), 137.53 (C3), 131.72 (C4), 149.08 (C5), 138.05 (C8), 129.16 (C9, C13), 127.97 (C10, C12), 131.06 (C11).

2.4.2. Synthesis of $[\text{Zn}(\text{pbth})_2]$

A methanol-acetonitrile solution (20 ml, 1:1 v/v) of the ligand N-picolinoyl-N'-benzothioylhydrazide (2 mmol) was added slowly to the methanol (10 mL) solution of $\text{Zn}(\text{OAc})_2 \cdot 2\text{H}_2\text{O}$ (1 mmol), stirred for 2 h, and then refluxed for 1h at 60 °C. A clear solution thus obtained was filtered and kept for crystallization. Crystals suitable for X-ray analyses were obtained by slow evaporation of the above solution over a period of 25 days. Yield: 56 %; m.p. 236 °C. Anal. Found: C, 53.96; H, 3.47; N, 14.58; S, 11.05 %. Calc. for $\text{C}_{26}\text{H}_{20}\text{ZnN}_6\text{S}_2\text{O}_2$ (578.01): C, 53.98; H, 3.46; N, 14.53; S, 11.07 %. IR (KBr, cm^{-1}): $\nu(\text{NH})$ 3284, $\nu(\text{C}=\text{O})$ 1621, $\nu(\text{N}-\text{N})$ 1090, $\nu(\text{C}=\text{S})$ 918, (Zn-N) 508, (Zn-S) 421. ^1H NMR (DMSO- d_6 ; δ ppm): 10.00 (s, 1H, NH), 8.24 (C1H), 8.13 (C2H), 7.91 (C3H), 8.14 (C4H), 7.51 (C9H), 7.34 (C10H), 7.32 (C11H), 7.25 (C12H), 7.49 (C13H). ^{13}C NMR (DMSO- d_6 ; δ ppm): 185.88 (C=S), 162.14 (C=O), 146.14 (C1), 131.75 (C2, C11), 136.63 (C3), 128.77 (C4), 148.50 (C5), 138.84 (C8), 127.16 (C9, C13), 126.43 (C10, C12).



Scheme 1 Synthesis of the ligand and its Zn(II) complex

3. Crystal structure determination

The X-ray data collection for the complex were performed on an Oxford Diffraction Gemini diffractometer equipped with CrysAlis Pro., using a graphite mono-chromated Mo K α ($\lambda = 0.71073 \text{ \AA}$) radiation source. The structures were solved by direct method (SHELXL-2008) and refined against all data by full matrix least-squares on F^2 using anisotropic displacement parameters for all non-hydrogen atoms. All the hydrogen atoms were included in the refinement at geometrically ideal positions and refined with a riding model [17]. The MERCURY package and ORTEP-3 programs were used for generating molecular structures [18, 19].

4. Quantum chemical calculation

The calculations based on DFT have been applied in many areas and the results also are in great agreement with the experimental ones in calculating spectroscopic properties [20]. The purpose of the present study is to compare the experimental data with theoretical and to calculate optimal molecular geometry of N-picolinoyl-N'-benzothioylhydrazide and its Zn(II) complex. All calculations were performed using the Gaussian 03 and Gauss View 4.1 [21] program. The

structure optimization of N-picolinoyl-N'-benzothioylhydrazide has been done using DFT method with functional B3LYP and basis set 6-311G(d,p) [22] whereas the geometry optimization for the complex has been done using DFT method with functional B3LYP and basis sets 6-311G(d,p){C,H,N,O,S}/Lanl2DZ. The basis set Lanl2DZ [23] serves the purpose of including the pseudo potential of the core electrons in the metal atoms. The input geometries of the zinc complex of N-picolinoyl-N'-benzothioylhydrazide for the DFT calculations were generated from single crystal X-ray data. The results obtained from theoretical calculations and experiments have been compared. The first task for the computational work was to determine the optimized geometry of N-picolinoyl-N'-benzothioylhydrazide and the Zn(II) complex. Analytic frequency calculations at the optimized geometry were done to confirm the optimized structures to be an energy minimum. At the optimized geometry for the N-picolinoyl-N'-benzothioylhydrazide and the Zn(II) complex, no imaginary frequency modes were obtained, so there is a true minimum on the potential energy surface is found. It is well known in the quantum chemical literature that the hybrid B3LYP method based on Becke's three parameter functional of DFT [24] yields a good description of harmonic vibrational wave numbers. This method is based on fairly large and flexible basis set 6-311G(d,p){C,H,N,O,S}/Lanl2DZ level to perform accurate calculations on the molecule were chosen. The HOMO-LUMO energies were calculated using B3LYP method of the DFT. In order to show NLO activity of the Zn(II) complex, the dipole moment, linear polarizability and first hyperpolarizability were obtained using the same level of theory.

5. Results and discussion

The ligand N-picolinoyl-N'-benzothioylhydrazide (Hpbth) reacts with $\text{Zn}(\text{OAc})_2 \cdot 2\text{H}_2\text{O}$ to give $[\text{Zn}(\text{pbth})_2]$ and is stable towards air and moisture. The ligand and the complex melt at 184 and

236 °C, respectively. The Scheme 1 depicts the formation of the ligand and Zn(II) complex. The colorless Zn(II) complex is insoluble in water, partially soluble in ethanol but highly soluble in chloroform, acetone and DMSO. In complex, the Zn(II) ion is coordinated through pyridyl nitrogen, hydrazinic nitrogen and thione sulphur of the ligand. Composition and identity of the assembled system were deduced from elemental analysis and IR, NMR, UV-vis and TGA.

5.1. IR spectra

The IR spectrum of the ligand N-picolinoyl-N'-benzothioylhydrazide (Hpbth) shows absorptions due to the stretching modes of NH (3236); C=O (1702); C=S (921) and N-N 1042 cm^{-1} . The IR spectrum of the $[\text{Zn}(\text{pbth})_2]$ shows the absence of $\nu(\text{NH})$ band together with the appearance of two new bands for $\nu(\text{Zn-N})$ and $\nu(\text{Zn-S})$ at 508 and 421 cm^{-1} respectively which suggests bonding of Zn(II) with hydrazine nitrogen [25]. The $\nu(\text{C=S})$ band suffers a negative shift of 53 cm^{-1} , indicating that pbth is acting as uninegative tridentate ligand, bonding through thione sulfur. The bonding through thione sulphur and hydrazinic nitrogen in the Zn(II) complex is further supported by X-ray crystallography.

5.2 ^1H and ^{13}C NMR spectra

The ^1H NMR spectrum of Hpbth exhibits two signals at δ 10.63 and 10.05 ppm for the amide and thioamide protons, respectively. Aromatic protons appear as multiplet between δ 7.2-8.8 ppm. The ^{13}C NMR spectrum of Hpbth shows two signals for two carbon atoms of which the signals at δ 190.71 and 163.07 ppm are due to the $>\text{C=S}$ and $>\text{C=O}$, carbons, respectively. The aromatic carbons appear at δ 122.62-149.08 ppm. The ^1H NMR spectrum of $[\text{Zn}(\text{pbth})_2]$ exhibits one signal at δ 10.00 ppm for the thioamide proton and the loss of amide proton indicates bonding of amide nitrogen to the zinc ion. Aromatic protons appear as multiplet between δ 7.25-8.24 ppm. The ^{13}C NMR spectrum of $[\text{Zn}(\text{pbth})_2]$ shows several signals for various carbon

atoms out of which the signals at δ 203.12 and 163.90 ppm are due to the $>C=S$ and $>C=O$, carbons, respectively. The signals appearing between δ 119.65-150.88 ppm are due to aromatic carbons.

5.3. Solid state electrical conductivity

Zn(II) complex shows solid state electrical conductivity at room temperature. Fig.1 shows that $\log \sigma$ of the complex decreases with increase in $1000/T$, indicating semiconducting behaviour. This may be due to the inclusion of zinc(II) ion in to the π electron delocalization of N-picolinoyl-N'-benzothioylhydrazide on complexation by the production of charge carriers which may take place *via* C-H $\cdots\pi$ interactions (Fig.4) [26, 27]. The band gap evaluated from the plot was found to be 0.64 eV for the Zn(II) complex, respectively. Furthermore, lower conductivity of the complex shows weaker inter-molecular contact and less extended delocalization and rules out any possibility of partial oxidation of the central metal and also the unpaired electrons are not participating in the electron conduction mechanism [28].

5.4. Antibacterial activity

Antibacterial activity of N-picolinoyl-N'-benzothioylhydrazide, $Zn(OAc)_2 \cdot 2H_2O$ and zinc(II) complex and commercial antibacterial drugs streptomycin sulphate and neomycin sulphate were tested against five human bacterial pathogens *Salmonella typhi* (MTCC 3216), *Shigella flexneri* (ATCC 12022), *Staphylococcus aureus* (ATCC 25323), *Aeromonas hydrophila* (ATCC 7966) and *Enterococcus faecalis*. The inhibition zones are given in the Table 1. The ligand and the complex were found active against all pathogens at higher concentration. The highest zone of inhibition (1.4 cm) was recorded in case of the complex against *Shigella flexneri* at 50 μ g/disc. The ligand shows little activity against *S. flexneri* and *A. hydrophila* at 30 μ g/disc but is more active at 50 μ g/disc in other cases. The result of antibacterial activity is also expressed as Mean \pm

standard deviation (SD) at the concentration range 30-50 $\mu\text{g}/\text{disc}$, [Table 2]. On comparing the inhibitory activity it is found that the Zn(II) complex is more effective than that of free ligand and $\text{Zn}(\text{OAc})_2 \cdot 2\text{H}_2\text{O}$. The order of activity is Zn(II) complex > Hpbth (ligand) > $\text{Zn}(\text{OAc})_2 \cdot 2\text{H}_2\text{O}$. Activity of the ligand and the Zn(II) complex are lower as compared to streptomycin sulphate and neomycin sulphate. It is clear that the zone of inhibition area is somewhat larger for the complex than those of the ligand and zinc acetate salt. Such increased activity of the metal chelate can be explained on the basis of chelation theory. On chelation, the polarity of the metal ion is reduced to a great extent due to the overlap of the ligand orbital. Furthermore, it increases the delocalization of π -electrons over the whole chelate ring and enhances the lipophilicity of the complex [29, 30]. This increased lipophilicity leads to breakdown of the permeability barrier of the cell and thus retards the normal cell processes [31] and show enhance antibacterial activity. Thus, the zinc complex may serve as moderate therapeutic agent antibacterial activity.

5.5. Thermal analysis

The thermal stability of the Zn(II) complex was studied by heating the sample at a control rate of 15 $^\circ\text{C}$ per minute under nitrogen atmosphere. The complex is stable up to 200 $^\circ\text{C}$, indicating the absence of lattice water as well as coordinated water [32]. Generally in TGA, lattice water loss occurs at low temperature in the range 60-120 $^\circ\text{C}$, whereas coordinated water requires a temperature in the range 120-230 $^\circ\text{C}$. Absence of water molecule in Zn(II) complex is supported by the DTA curve also, which represents weight loss by endothermic process [33]. Thermogravimetric analysis of zinc(II) complex shows that the complex starts decomposing above 200 $^\circ\text{C}$ and thermogram exhibits two distinct decompositions at 200 and 480 $^\circ\text{C}$. The first weight loss (Cald; 68.16%, Obs; 67.55%) could be due to loss of two picolinamide molecule along with two phenyl molecule and a corresponding endothermic peak at 223 $^\circ\text{C}$ was obtained.

The second decomposition between 480 to 700 °C shows the weight loss (Cald; 16.31%, Obs; 16.36 %) and endothermic peak observed at higher temperature in DTA is due to loss of organic moieties in the form of gaseous product and finally metal is converted into its oxide [34]. In addition to endothermic peaks, the DTA curve of the complex also shows exothermic peaks which appear at high temperature and represent oxidation and/or decomposition of the complex. The thermogravimetric curve for the complex is presented in Fig 2.

5.6. Crystal structure description

Fig. 3 shows the ORTEP diagram of the complex $[\text{Zn}(\text{pbth})_2]$ together with the atom numbering scheme. The crystallographic data and structural refinement details for **1** are given in Table 3 and selected bond distances and bond angles of the complex are compiled in Table 4 and hydrogen bonding parameters in Table 5. The complex $[\text{Zn}(\text{pbth})_2]$ contains a pair of N-picolinoyl-N'-benzothioylhydrazide ligand coordinated to Zn(II) ion *via* thione sulphur, pyridyl nitrogen and hydrazinic nitrogen forming two five membered chelate rings. The C=O bond length [1.238(5) Å] is purely a double bond which remains uncoordinated but takes part in the formation of supramolecular architecture through hydrogen bonding [35, 36]. The C7-S1 bond distance present in the both units of the ligand is 1.678 (4) Å which suggest that it is intermediate between single and double bond [37]. The complex may be described to have a distorted octahedral geometry with the ligand-metal-ligand angle varying between 81.10(10) [N(2)-Zn(1)-S(1)] to 77.65(14) [N(2)-Zn-N(1)] in the chelate rings. The average bond lengths of N2-N3 = 1.387, N3-C7 = 1.315, C7-S1 = 1.678 Å and N1-C5 = 1.344, C5-C6 = 1.491, C6-N2 = 1.322 Å, suggest considerable delocalization of charge in the both five membered chelate rings [38]. The dihedral angles formed between the pyridine and the phenyl ring is found to be 77.35° which suggest that the two rings are nearly perpendicular to each other. The structure of the complex is

stabilized by N-H...O intermolecular hydrogen bonding occurring between the carbonyl oxygen and hydrogen of hydrazinic nitrogen and C-H...O intermolecular hydrogen bonding between carbonyl oxygen and phenyl hydrogen. In addition, the C-H... π interactions at a distances of 2.855 and 3.638 Å act as a linker between two units of the ligand molecule in the formation of supramolecular architecture (Fig. 4). Furthermore, the crystal packing shows that both sulphur atoms of each molecule in every row are arranged in such a way that they face each other (Fig.5).

5.7. DFT calculations of *N*-picolinoyl-*N'*-benzothioylhydrazide (*Hpbth*) and its Zn(II) complex

The optimized geometrical parameters are listed in Table 4. The optimized energy of *Hpbth* and Zn(II) complex are -1134.3745 and -1566.9097 a.u respectively indicating that the complex is more stable than the ligand. The optimized geometry of complex accounts for distorted octahedral geometry with Zn-N, Zn-S and Zn-N_{py} bond distances of 1.981, 2.454 and 2.127 Å, respectively. The C=O and C-S bond lengths 1.236 and 1.671 Å accounts for double and single bond character and N_{hy}-Zn-N_{py} and N_{hy}-Zn-S chelate angles are 77.627 and 81.117 °, respectively. The slight disagreement in the bond lengths is due to the fact that the DFT calculations are done for an isolated molecule in gaseous phase while the X-ray crystallographic data were obtained from crystal lattice of complex molecules [39, 40]. The optimized geometries of *Hpbth* and the Zn(II) complex along with the atomic labelling scheme are shown in Fig 6a and 7a. As it can be seen from the experimental results that the most probable coordination site are N, S and O atom which are also verified by theoretical calculations of optimized complexes. There is good agreement between the geometrical parameters obtained by X-ray crystallography to those generated by DFT method as shown in Table 4. The charge distribution on atoms of *Hpbth* and its Zn(II) complex are also calculated and the charges on the ligand decreases, as a result of redistribution on complexation [41]. The negative charges on binding atoms shift to

lower values: N_{pyridyl} (-0.482 to -0.185), $N_{\text{hydrazine}}$ (-0.375 to -0.318) and S_{thione} (-0.148 to 0.021) which indicates that the charge redistribution takes place after complex formation.

5.8. Molecular electrostatic potential and Contour maps:

To predict reactive sites [42] for electrophilic and nucleophilic process for the ligand (Hpbth), electrostatic surface potentials were obtained at the B3LYP/6-311G(d,p) optimized geometry. The MEP mapped surface of the molecule are calculated by DFT/B3LYP/6-311G(d,p){C,H,N,O,S}/Lanl2DZ method at the 0.02 isovalues and 0.004 density values. The red colour scheme of MEP is the negative electrostatic potentials. The red region show atoms with lone pairs; the intensity of the colour is proportional to the absolute value of the potential energy. The positive electrostatic potentials are shown in blue colour region which characterize the C-H bonds. The yellow/green areas cover parts of the molecule where electrostatic potentials are close to zero (C-C, C-N and C-S bonds). The MEP mapped surface for Hpbth and the Zn(II) complex are shown in Figs 6b and 7b. The negative red regions of MEP are related to electrophilic reactivity and the positive (blue) ones to nucleophilic reactivity. As can be seen from the figures, this molecule has several possible sites for electrophilic attack [43]. Negative regions in the Hpbth were found around the thione S, carbonyl oxygen, hydrazinic and pyridyl nitrogens. Thus, it would be predicted that an electrophile would preferentially attack to the ligand Hpbth at the O, S and N positions. According to the calculated results, the MEP map shows that the negative potential sites are on electronegative oxygen, sulphur and nitrogen atoms as well as the positive potential sites are around the hydrogen atoms. These sites give information about the region from where the compound can have noncovalent interactions. A contour plot or map is a two-dimensional plot of a three-dimensional surface showing lines where the surface intersects planes of constant elevation (Z) and is used to show lines of constant

density or brightness, such as electrostatic potentials. The contour maps are also calculated by DFT/B3LYP/6-311G(d,p) {C,H,N,O,S}/Lan12DZ method at the 0.02 isovalue and 0.004 density values at same level of calculations of the MEP mapped surface of the molecules. The contour maps of the molecules are shown in Fig 6c and 7c. The red lines are more around thione sulphur, hydrazinic and pyridyl nitrogens than on carbonyl side. Hence, the positive zinc(II) ions preferably bind through the thione sulphur, hydrazine and pyridyl nitrogen. The red lines decreases after complexation.

5.9. Frontier molecular orbitals and NLO analysis

The Fig. 6d and 7d show distribution and energy levels of the HOMO and LUMO orbitals computed at the B3LYP/6-311G(d) level for the ligand and Zn(II) complex. As seen from (Fig.1d), the HOMO of the ligand, electrons are localized on the thione sulphur with $E_{\text{HOMO}} = -8.0344$ eV. For the LUMO, electrons are mainly localized on the pyridyl nitrogen with $E_{\text{LUMO}} = -2.9989$ eV. The value of the energy separation between the HOMO and LUMO is 5.0355 eV. Whereas for HOMO of Zn(II) complex, electrons are mainly delocalized on the carbonyl oxygen, hydrazinic nitrogen and thione sulphur with $E_{\text{HOMO}} = -5.4657$ eV and for LUMO, electrons are delocalized on the carbonyl oxygen, hydrazinic nitrogen, thione sulphur and pyridyl ring nitrogen with $E_{\text{LUMO}} = -1.8833$ eV and the energy gap is 3.5824 eV. This small HOMO–LUMO energy gap means low excitation energy for the complex, a good stability and a low chemical hardness for the complex than the ligand [44]. The molecules having a large energy gap are known as hard, and molecules having a small energy gap are known as soft molecules. The soft molecules are more polarizable than the hard ones, because they need small energy for excitation. The hardness value of a molecule can be determined by the formula [45]

$$\eta = \{-E_{\text{HOMO}} + E_{\text{LUMO}}\}/2$$

where E_{HOMO} and E_{LUMO} are the energies of the HOMO and LUMO molecular orbitals. The value of η (Table 6) of Hpbth and the Zn(II) complex, are 2.51775 and 1.79120 eV, respectively indicates that the Zn(II) complex is a soft material than the ligand Hpbth.

The non-linear optical (NLO) properties of materials associated with the delocalized π -electrons of a molecule play an important role in the design of materials used in communication technology and optical devices [46]. An increase in delocalization of electron on the molecule is resulted in the change in the NLO properties which in turn are related to the energy gap between HOMO and LUMO. An addition of substituent to the conjugated systems or intermolecular hydrogen bonding, could affect the nonlinear optical properties by changing the energy gap between HOMO and LUMO where the small HOMO-LUMO gap requires small excitation energy and so the absorption bands of a molecule are shifted towards the visible region [47]. Due to the presence of various types of hydrogen bonding and $\text{CH}\cdots\pi$ interaction in Zn(II) complex, electron delocalization becomes easier, which decreases the value of the energy gap, so the absorption bands in the electronic spectrum of complex is shifted towards the visible region and consequently, increases the nonlinear optical properties as compared to Hpbth. This suggests that the metal modify the charge distribution of the π -electronic structure versus that of the free ligand Hpbth. Further the calculated hardness value of complex indicates for soft material and first hyperpolarizability (β_{tot}) value for the complex (10.827×10^{-30} esu), indicates for the complex to be a potential applicant in the development of NLO materials [48].

6. Conclusion

The ligand N-picolinoyl-N'-benzothioylhydrazide (Hpbth) and its complex $[\text{Zn}(\text{pbth})_2]$ have been synthesized and characterized by various physicochemical methods. Crystal structure of the complex is stabilized through weak intermolecular $\text{N-H}\cdots\text{O}$ and $\text{C-H}\cdots\text{O}$ interactions between

hydrogens of hydrazine nitrogen and phenyl ring with carbonyl oxygen. Also the crystal structure of the complex is stabilized by $\text{CH}\cdots\pi$ interactions occurring between phenyl hydrogens with π electrons of adjacent phenyl ring. The presence of $\text{C-H}\cdots\pi$ interaction at a short distance of 2.855 Å may be responsible for semiconducting behaviour of the Zn(II) complex. The Hpbth and Zn(II) complex are found to be active against all the test pathogens at higher concentration. TGA shows that the complex is stable up to 200 °C, indicating the absence of lattice water as well as coordinated water and finally zinc oxide is left as the residue. The optimized energy of Hpbth and Zn(II) complex is -1134.3745 and -1566.9097 a.u, respectively, indicating that the complex is more stable than the ligand. MEP map and contour plot shows the negative potential sites are on oxygen, sulphur and nitrogen atoms and the positive potential sites are around the hydrogen atoms. Hence, the positive zinc(II) ions preferably bind through the thione sulphur, hydrazine and pyridyl nitrogen sides thereby forming stable five membered chelate ring. The nonlinear optical property is addressed theoretically and the complex may be a potential applicant in the development of NLO materials.

7. Acknowledgements

Dr. S.K. Kushawaha is thankful to the Department of Science and Technology, New Delhi, India for the award of a Young Scientist Project (No. SR/FT/CS-110/2011). R.K. Dani thanks to UGC, New Delhi for the award of RGNF (SRF).

8. Supplementary material

CCDC 948488 contains the supplementary crystallographic data for $[\text{Zn}(\text{pbth})_2]$ These data can be obtained free of charge *via* <http://www.ccdc.cam.ac.uk/conts/retrieving.html>, or from the Cambridge Crystallographic Data Center, 12 Union Road, Cambridge CB2 IEZ, UK; fax: (+44)1223-336-033; or e-mail: deposit@ccdc.cam.ac.uk.

References

- [1.] A. Bacchi, A. Bonini, M. Carcelli, F. Ferraro, E. Leporati, C. Pelizzi, G. Pelizzi, *J.Chem. Soc., Dalton Trans.* (1996) 2699-2704.
- [2.] M. Carcelli, D. Delledonne, A. Fochi, G. Pelizzi, M.C. Rodriguez-Arguelles, U. Russo, *J. Organomet. Chem.* 544 (1997) 29-35.
- [3.] B. Moubaraki, K.S. Murray, J.D. Ranford, X. Wang, Y. Xu, *Chem. Commun.* (1998) 353-354.
- [4.] A. Shrivastava, N.K. Singh, S.B. Singh, S.M. Singh, N. Singh, A. Shanker, *Bioinorg.Chem. Appl.* 1 (2003) 255-270.
- [5.] N.K. Singh, S.B. Singh, *Transition Met. Chem.* 26 (2001) 487-495.
- [6.] M. Patil, R. Hunoor, K. Gudasi, *Eur. J. Med. Chem.*, 45(2010), 2981-2986.
- [7.] Z.H. Chohan, S.H. Sumrra, M.H. Youssoufi, T.B. Hadda, *Eur. J. Med. Chem.*, 45(2010), 2739-2747.
- [8.] A .E. Liberta, D.X. West, *BioMetals* 5 (1992) 121-126.
- [9.] D.X. West, A.E. Liberta, S.B. Padhye, R.C. Chikate, P.B. Sonawane, A.S. Kumbhar, R.G. Yerande, *Coord. Chem. Rev.* 123 (1993) 49-53.
- [10.] R.L. Dutta, Md.M. Hossain, *J. Sci. Ind. Res.* 44 (1985) 635-674.
- [11.] B. Moubaraki, K. S. Murray, J. D. Ranford, J. J Vittal, X. Wang, Y. Xu, *Chem. Soc. Dalton Trans.* (1999) 3573-3578.
- [12.] H. Cheng, D. Chun-ying, F. Chen-Jie, L. Yong-jiang, M. Qing-jin, *J. Chem. Soc. Dalton Trans.* (2000) 1207-1212.
- [13.] N.K. Singh, A.K. Srivastava, P. Tripathi, A. Shrivastava, R.K. Sharma, *Eur.J.Med. Chem.*43 (2008) 577-583.
- [14.] A.W. Bauer, W.M. Kirby, J.C. Sherris, M. Turck *Am J. Clin. Pathol.* 45 (1966), 493-496.

- [15.] S. K. Gond, Mishra A. V.K. Sharma, S.K. Verma, J. Kumar, R.N. Kharwar, A. Kumar, *Mycoscience* 53 (2012), 113-121.
- [16.] N.K. Singh, D.K. Singh, S. B. Singh *Synth. React. Inorg.Met.-Org. Chem* 32 (2002) 703-720.
- [17.] G.M. Sheldrick, *Acta Crystallogr., Sect. A* 64 (2008) 112.
- [18.] I.J. Bruno, J.C. Cole, P.R. Edgington, M. Kessler, C.F. Macrae, P. McCabe, J. Pearson, R. Taylor, *Acta Crystallogr., Sect. B* 58 (2002) 389.
- [19.] L.J.J. Farrugia, *Appl. Crystallogr.* 30 (1997) 565.
- [20.] Y. Zhang, Z.J. Guo, X.Z. You, *J. Am. Chem. Soc.* 123 (2001) 9378–9387.
- [21.] M.J. Frisch, G.W. Trucks, H.B. Schlegel, G.E. Scuseria, M.A. Robb, J.R. Cheeseman, V.G. Zakrzewski, J.A. Montgomery, R.E. Stratmann, J.C. Burant, S. Dapprich, J.M. Millam, A.D. Daniels, K.N. Kudin, M.C. Strain, O. Farkas, J.B. V. Tomasi, M. Cossi, R. Cammi, B. Mennucci, C. Pomelli, C. Adamo, S. Clifford, J. Ochterski, G.A. Petersson, P.Y. Ayala, Q. Cui, D.K. Morokuma, A.D. Malick, K. Rabuck, J.B. Raghavachari, J. Foresman, J.Cioslowski, J.V. Ortiz, A.G. Baboul, B.B. Stefanov, G.L.A. Liu, P. Piskorz, I. Komaromi, R. Gomperts, R.L. Martin, D.J. Fox, T. Keith, M.A. Al-Laham, C.Y. Peng, A. Nanayakkara, M. Challacombe, P.M.W. Gill, B. Johnson, W. Chen, M.W. Wong, J.L. Andres, C. Gonzalez, M. Head-Gordon, E.S. Replogle, J.A. Pople, *Gaussian 03, Revision A.1*, Gaussian, Inc., Pittsburgh, 2003.
- [22.] A.D. Becke, *J. Chem. Phys.* 98 (1993) 5648-5652.
- [23.] C. Lee, W. Yang, R.G. Parr, *Phys. Rev. B.* 37 (1988) 785-789.
- [24.] M.A. McAllister, *Theochem* 427 (1998) 39-53.
- [25.] K. Nakamoto, *Infrared and Raman Spectra of Inorganic and Coordination Compounds*, 4th ed., Wiley Interscience, New York, 1986.

- [26.] M. G. A. E. Wahed, A. M. Hassan and S. A. Hassan, *J. Mater. Sci. Lett.*, 12 (1993) 453-454.
- [27.] R.K. Dani, M.K. Bharty, S.K. Kushawaha, Om Prakash, R.K. Singh, N.K. Singh., *Polyhedron* 65 (2013) 31-41.
- [28.] N.K. Singh, S.K. Kushawaha, *Trans. Met. Chem.* 26 (2001) 140-146.
- [29.] R. S. Srivastava, *Inorg. Chim. Acta.* 56 (1981), 65-67.
- [30.] N. Gupta, R. Swaroop, R. V. Singh, *Main Group Met. Chem.* 14 (1997), 387-390.
- [31.] W.E Levinson, E. Jawetz, *Medical Microbiology and Immunology*, 4th edit., Stamford, 1996.
- [32.] A.H. Kianfar, L. Keramat, M. Dostani, M. Shamsipur, M. Roushani, F. Nikpour, *Spectrochem. Acta A* 77 (2010) 424-429.
- [33.] A. Anthonysamy, S. Balasubramanian, *Inorg. Chem. Commun.* 8 (2005) 908-911
- [34.] A.V. Nikolaev, V.A. Logvienko, L.T. Myachina, *Thermal analysis Vol. 2*, (Academic Press, New York 1969) 779.
- [35.] T.S. Lobana, G. Bawa, A. Castineiras, R.J. Butcher, *Inorg. Chem. Comm.*, 10 (2007) 506-509.
- [36.] T.S. Lobana, P. Kumari, R.J. Butcher, T. Akitsu, Y. Aritake, J. Perles, F.J. Fernandez, M.C. Vega, *J. Organomet. Chem.*, 701 (2012) 17-26.
- [37.] L.E. Sutton, *Tables of Interatomic Distances and Configuration in Molecules and Ions*, Special Publication No. 18. The Chemical Society, London, 1965.
- [38.] J. R. Dilworth, J. Hyde, P. Lyford, P. Vella, K. Venkatasubramaman, J.A. Zubieta, *Inorg. Chem.*, 18 (1979) 268.
- [39.] A.D. Becke, *J. Chem. Phys.* 98 (1993) 5648-5652.

- [40.] R. Gupta, R.P. Chaudhary, *J. Mol. Struct.* 1049 (2013) 189-197.
- [41.] Om Prakash, S.K. Singh, B. Singh, R.K. Singh, *Spectrochimica Acta Part A* 112 (2013) 410-416.
- [42.] J.S. Murray, K. Sen, *Molecular Electrostatic Potentials, Concepts and Applications*, Elsevier, Amsterdam, 1996.
- [43.] M. Govindarajan, M. Karabacak, A. Suvitha, S. Periandy, *Spectrochimica Acta Part A* 89 (2012) 137-148.
- [44.] M. Arivazhagan, R. Meenakshi, *Spectrochim. Acta* 91A (2012) 419-430.
- [45.] K. Fukui, *Science* 218 (1982) 747-754.
- [46.] D. Sajan, J. Hubert, V.S. Jayakumar, J. Zaleski, *J. Mol. Struct.* 785 (2006) 43-53.
- [47.] R.G. Pearson, *Proc. Natl. Acad. Sci.* 83 (1986) 8440-8441.
- [48.] H. Tanak, M. Toy, *Spectrochimica Acta Part A* 115 (2013) 145-153.

Table 1 Antibacterial assay of the Hpbth and [Zn(pbth)₂] against human bacterial pathogens

Test pathogen	Concentration of compound (µg/disc)	Compound			Standard drug		Control DMSO (10µl/disc)
		Hpbth	[Zn(pbth) ₂]	Zn(OAc) ₂ ·2H ₂ O	Streptomycin sulphate	Neomycin sulphate	
<i>Salmonella typhi</i> (MTCC 3216)	5	-	-	-	2.4	1.8	-
	10	-	-	-	2.5	1.9	
	20	-	0.6	0.1	2.7	2.0	
	30	0.5	0.7	0.2	2.8	2.1	
	40	0.6	0.8	0.4	2.9	2.2	
	50	0.7	1.0	0.6	3.0	2.4	
<i>Shigella flexneri</i> (ATCC 2022)	5	-	-	-	0.8	1.5	-
	10	-	-	-	1.0	1.8	
	20	-	0.8	0.3	1.6	2.0	
	30	0.3	0.9	0.4	2.0	2.1	
	40	0.5	1.0	0.6	2.3	2.2	
	50	0.6	1.4	0.7	2.5	2.5	
<i>Staphylococcus aureus</i> (ATCC 5323)	5	-	-	-	1.8	1.75	-
	10	-	-	-	2.0	1.8	
	20	-	-	0.2	2.3	1.9	
	30	-	0.7	0.3	2.4	2.1	
	40	0.5	0.8	0.4	2.5	2.2	
	50	0.6	0.9	0.6	2.8	2.3	
<i>Aeromonas hydrophila</i> (ATCC 7966)	5	-	-	-	2.5	1.75	-
	10	-	-	-	2.6	2.0	
	20	-	-	-	2.7	2.15	
	30	0.4	0.6	0.3	2.8	2.3	

	40	0.5	0.7	0.4	2.9	2.4	
	50	-	0.9	0.6	3.0	2.6	
<i>Enterococcus faecalis</i>	5	-	-	-	1.9	1.8	-
	10	-	-	-	2.2	1.9	
	20	-	-	0.1	2.5	2.0	
	30	0.5	0.6	0.3	2.6	2.1	
	40	0.7	0.8	0.4	3.0	2.3	
	50	0.8	1.1	0.7	3.2	2.5	

- No zone was observed, *inhibition zone is the average of the diameter of zone from two sides in cm.

Table 2 Inhibition zone of antibacterial activity for compounds

Conc. ($\mu\text{g}/\text{disc}$)	Zone of inhibition (mean \pm SD)		
	Ligand	Zn(OAc) $_2$ ·2H $_2$ O	[Zn(pbth) $_2$]
30	0.4 \pm 0.22	0.3 \pm 0.07	0.7 \pm 0.12
40	0.5 \pm 0.11	0.4 \pm 0.10	0.8 \pm 0.11
50	0.7 \pm 0.36	0.6 \pm 0.07	1.0 \pm 0.22

Table 3 Crystallographic data for [Zn(pbth)₂]

Empirical formula	C ₂₆ H ₂₀ N ₆ O ₂ S ₂ Zn
Formula weight	578.01
T (K)	293(2)
λ (Mo K α) (Å)	0.71073
Crystal system	Monoclinic
Space group	C 2/c
a (Å)	24.178(4)
b (Å)	8.9617(6)
c (Å)	15.381(3)
β (°)	129.49(3)
V (Å ³)	2572.0(13)
Z	4
D _{calc} (mg m ⁻³)	1.493
μ (mm ⁻¹)	1.154
F(000)	1184
Crystal size(mm ³)	0.27x0.24x0.22
θ range (°)	3.42-29.08
Index ranges	-32 ≤ h ≤ 32 -12 ≤ k ≤ 12 -19 ≤ l ≤ 21
Reflections collected	3563
Independent reflections	1898
Data/restraints/ parameters	2503/0/168
Goodness-of-fit on F ²	0.854
Final R indices wR_2 [$I > 2\sigma(I)$](R _{int})	0.0572, 0.1120
Final R indices (all data)	0.0892, 0.1340
Largest diff. peak/hole (e Å ⁻³)	0.659, -0.951

$${}^a R_1 = \frac{\sum ||F_o| - |F_c||}{\sum |F_o|}, \quad {}^b R_2 = \left[\frac{\sum w (|F_o|^2 - |F_c|^2)^2}{\sum w |F_o|^2} \right]^{1/2}.$$

Table 4 Selected bond lengths (Å) and bond angles (°) for [Zn(pbth)₂]

Bond lengths (Å)			Bond angles (°)		
	Exp.	Cal.		Exp.	Cal.
Zn-N2	1.982(4)	1.981	N2-Zn-N2	178.5(2)	178.519
Zn-N2	1.982(4)	1.981	N2-Zn-N1	77.65(14)	77.627
Zn-N1	2.128(4)	2.127	N2-Zn-N1	103.48(15)	103.493
Zn-N1	2.128(4)	2.127	N1-Zn-N1	84.98(19)	84.984
Zn-S1	2.454(13)	2.454	N2-Zn-S1	81.10(10)	81.117
Zn-S1	2.454(13)	2.454	N2-Zn-S1	97.85(12)	97.843
S1-C7	1.678(4)	1.671	N1-Zn-S1	95.56(10)	95.561
O1-C6	1.238(5)	1.236	N1-Zn-S1	158.24(11)	158.241
N2-C6	1.322(5)	1.322	S1-Zn-S1	91.87(7)	91.867

Table 5 Hydrogen bond parameters [\AA and $^\circ$] in $[\text{Zn}(\text{pbth})_2]$

D-H \cdots A	d(D-H)	d(H \cdots A)	d(D \cdots A)	$\angle(\text{DHA})$
Intermolecular hydrogen bond				
N3-H3A \cdots O1	0.860	1.911	2.766	172.78
C12-H12 \cdots O1	0.931	2.664	3.530	155.19
Intramolecular hydrogen bond				
N3-H3A \cdots O1	0.860	2.490	2.746	98.04
C4-H4 \cdots O1	0.931	2.572	2.836	96.72

Table 6 Calculated Frontier Molecular Orbital energies (eV) for Hpbth and complex [Zn(pbth)₂]

Molecule	Energies (ev)			Degree of Hardness η
	HOMO	LUMO	Energy Gap	
Hpbth	-8.0344	-2.9989	5.0355	2.51775
[Zn(pbth) ₂]	-5.4657	-1.8833	3.5824	1.79120

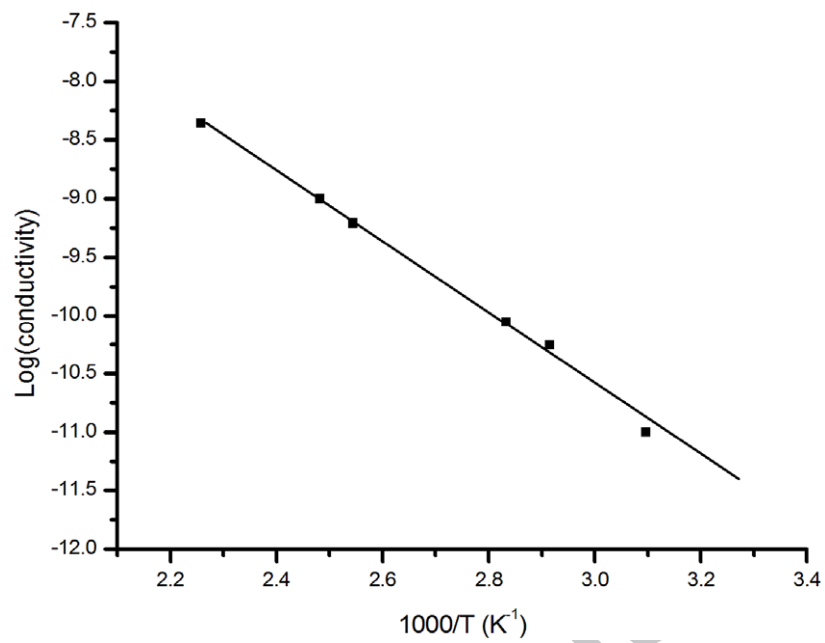


Fig. 1 Solid state electrical conductivity

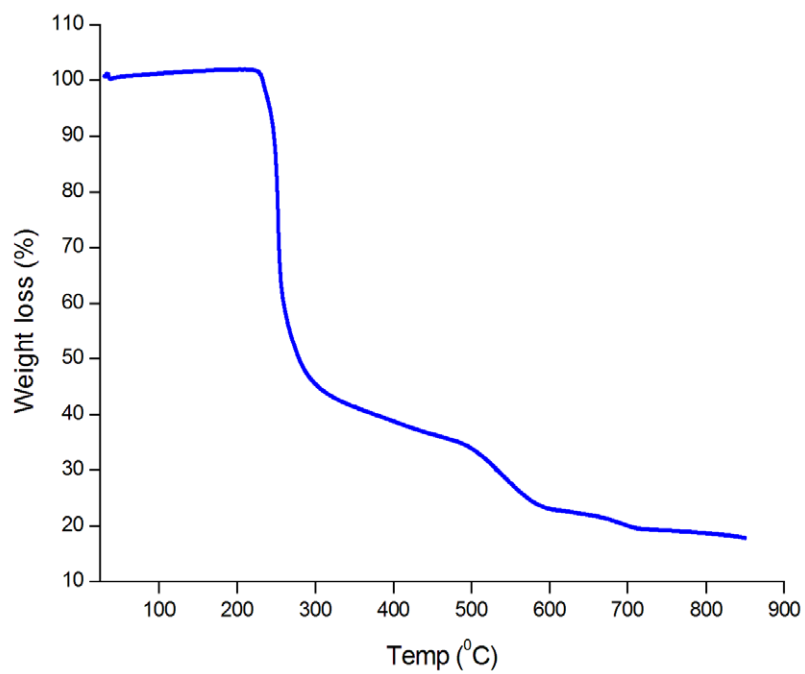


Fig. 2 Thermogram of Zn(II) complex

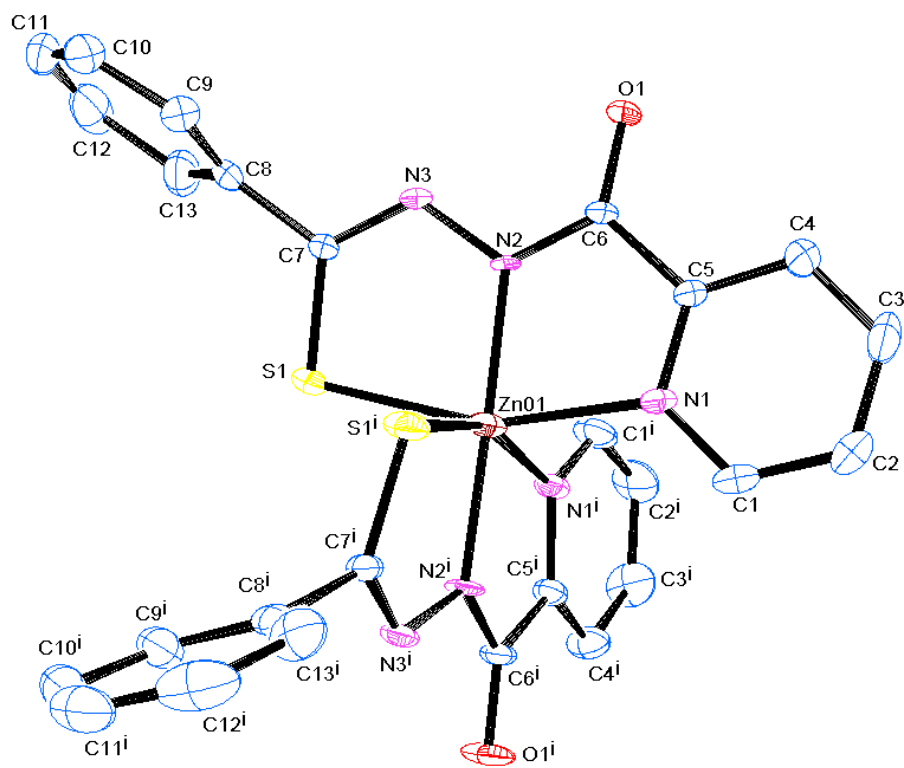


Fig.3 Ortep diagram of [Zn(pbth)₂]

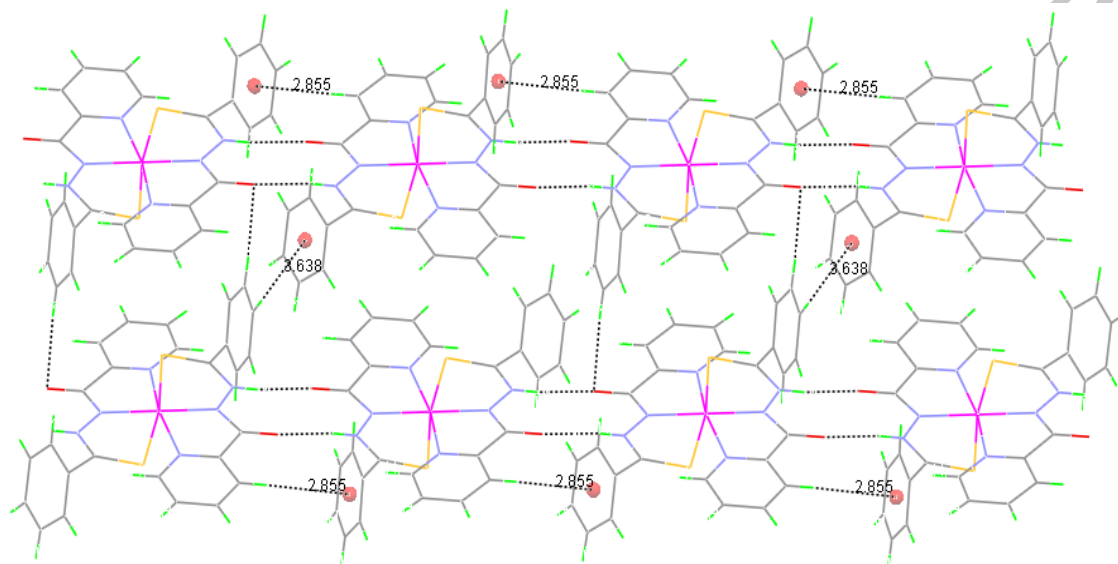


Fig.4 C-H...O, N-H...O and C-H... π interaction in Zn(II) complex, leading linear chain structure

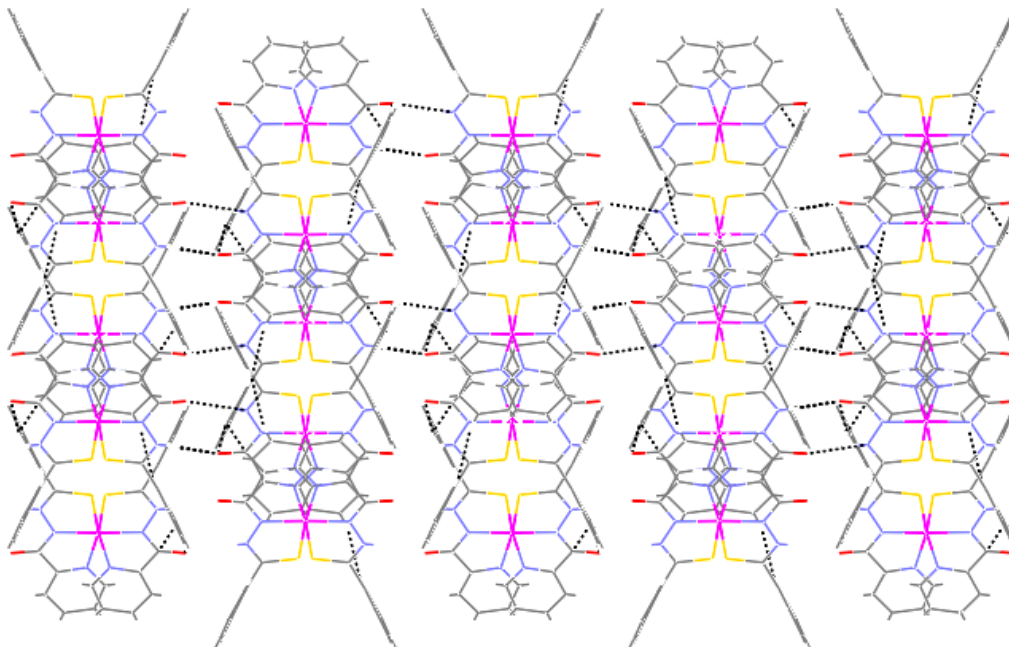


Fig.5 Crystal packing of Zn(II) complex along c axis

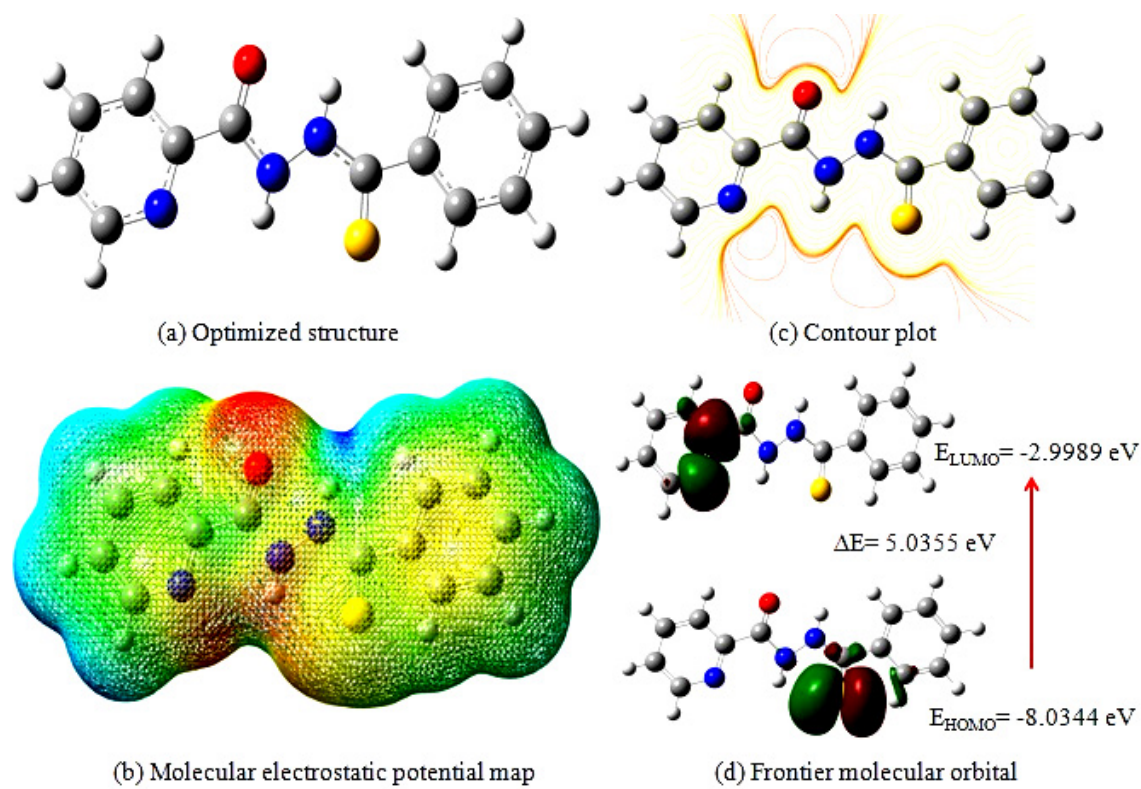


Fig. 6(a-d) DFT calculation of N-picolinoyl-N'-benzothioylhydrazide

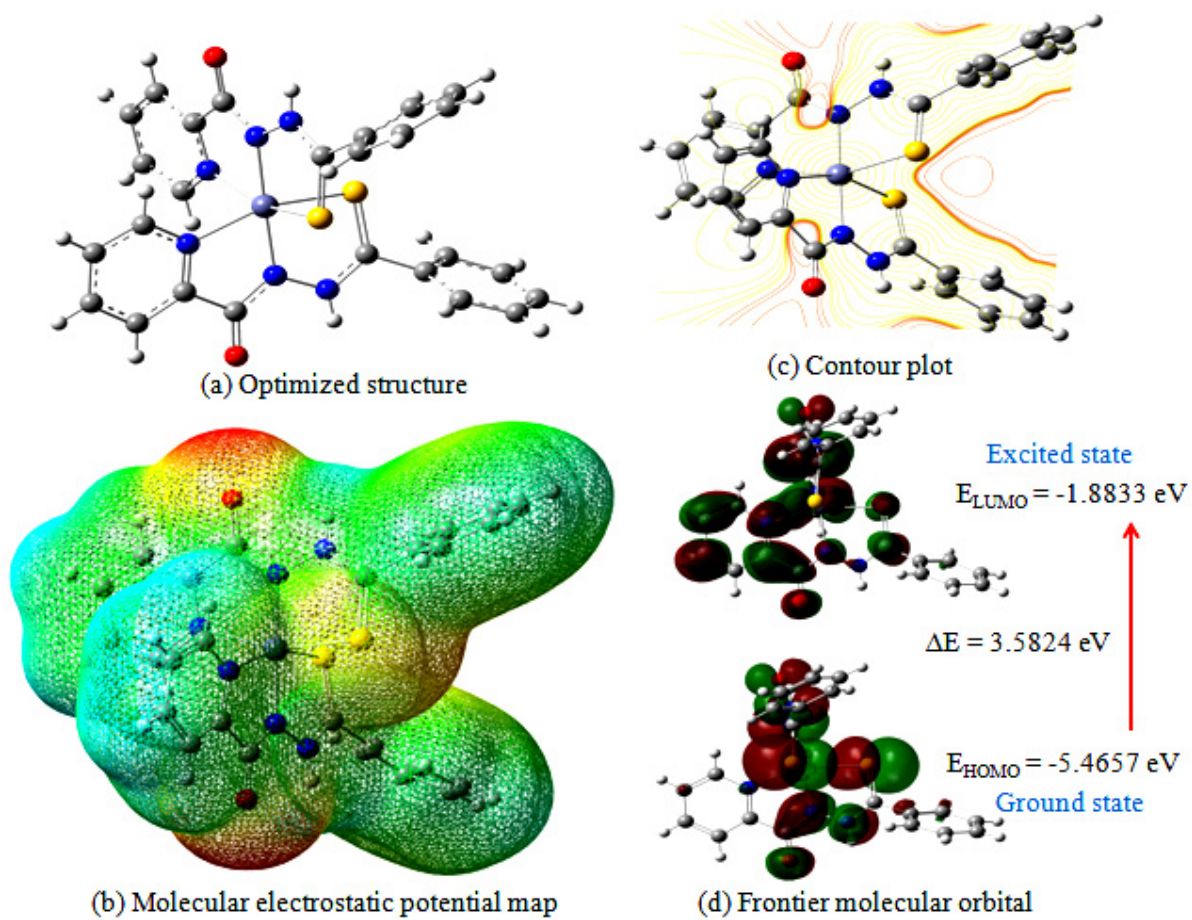
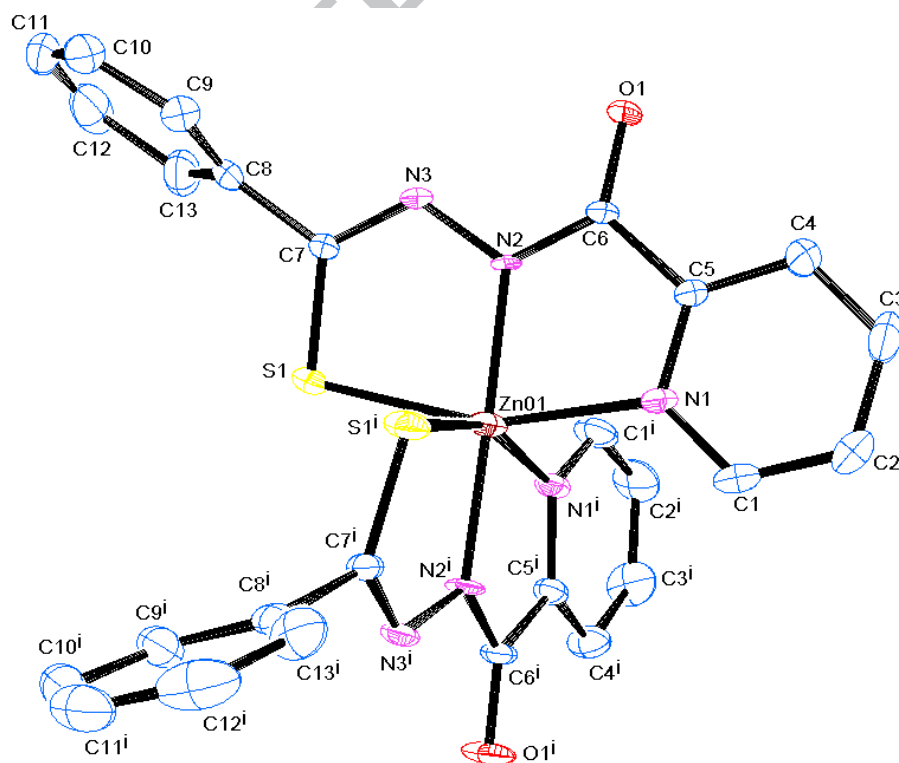


Fig. 7(a-d) DFT calculation of [Zn(pbth)₂]

Graphical Abstract

A new Zn(II) complex $[Zn(pbth)_2]$ (where Hpbth = N-picolinoyl-N'-benzothioyl hydrazide) has been synthesized and characterized by elemental analyses, IR, UV-Visible and single crystal X-ray data. The distorted octahedral complex is stabilized by various types of inter and intramolecular extended hydrogen bonding providing supramolecular framework. The results of the optimized molecular geometry are presented and compared with the experimental X-ray diffraction data. The solid state electrical conductivity and thermal behavior (TGA) of the complex were investigated. The bioefficacy of the complex has been examined against the growth of bacteria *in vitro* to evaluate their anti-microbial potential.



Research Highlights

- A new complex $[\text{Zn}(\text{pbth})_2]$ with N-picolinoyl-N'-benzothioylhydrazide has been reported.
- The complex is distorted octahedral involving NNS tridentate ligand.
- Structural data from X-ray are corroborated well with DFT calculations.
- The ligand and complex show antibacterial activity but lower than the standard drugs.
- Lower solid state conductivity of the complex shows weaker inter-molecular contact.

ACCEPTED MANUSCRIPT